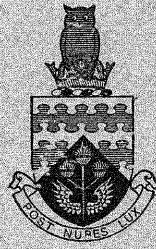


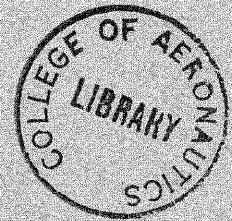
CoA/N/MAT-26

R 38,049/B

CoA NOTE MAT. No. 26



THE COLLEGE OF AERONAUTICS
CRANFIELD



SOME MICROSTRUCTURAL FEATURES OF FATIGUE
IN AN ALUMINIUM ALLOY

by

B. S. Hockenull, R. G. Hacking and J. D. Panakal

R 38,049/B



THE COLLEGE OF AERONAUTICS

DEPARTMENT OF MATERIALS

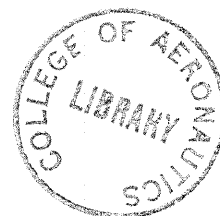
Some microstructural features of fatigue in an aluminium alloy

- by -

B.S. Hockenhull*

R.G. Hacking*

J.D. Panakal**



S U M M A R Y

The microstructures produced by the heat treatment of a commercial age-hardening Al-4.4 Cu alloy have been examined by thin foil electron microscopy. Whilst there is similarity of the microstructures in the commercial alloy to those which have been reported for simple binary Al-Cu alloys, there is a strong association of dislocation structures and incoherent precipitates with undissolved Mn bearing intermetallic particles.

Fatigue tests made on the alloy at both 50 Hz and 20 kHz have shown that there are changes in microstructure during fatigue, more markedly at 20 kHz in which tests the heating effect has some importance. There is some evidence of both accelerated ageing and also the by-passing or resolution of coherent phases during fatigue, particular at 20 kHz.

* The College of Aeronautics, Cranfield.

** Directorate of Naval Air Materials, Indian Navy, New Delhi.

Contents

	<u>Page No.</u>
1. Introduction	1
2. Experimental work	1
2.1 Material	1
2.2 Fatigue tests	1
2.3 Preparation of thin foils	2
3. Results	2
3.1 Fatigue tests	2
3.2 Examination of microstructures	3
3.2.1 Unfatigued material	3
3.2.2 Low frequency fatigued material	4
3.2.3 High frequency fatigued material	4
4. Discussion	5
4.1 Fatigue induced changes in microstructure	5
4.2 Discussion of results	6
5. Conclusions	9
6. Acknowledgements	10
7. References	10
Tables	12
Figures	

1. Introduction

Studies have been made recently on the fatigue properties of several commercial age-hardening aluminium alloys, with particular reference to the effect of high-frequency stressing at 20 kHz.^{1,2} The change in fatigue properties with frequency for the materials investigated, is that, at stresses above the fatigue limit, the number of cycles to failure is larger at high frequency, and most of the life is spent in initiation and early growth of the crack rather than in its propagation.

Since the frequency effect is not wholly environmental in nature,² it was necessary to examine and compare the microstructural features developed during fatigue stressing at high and low frequency. In addition, different heat treatment conditions have been found to produce smaller effects on the fatigue properties at low frequency than at high frequency, which suggests a variation in the interaction of the fatigue stressing with the precipitation processes in the material.^{1,3,4}

A good deal of information is available on the substructures of simple binary and ternary age-hardening aluminium alloys^{5,6} and on the effects of fatigue stressing on the substructures of pure metals and simple alloys^{7,8,9,10,11}. There is however, little published information on the microstructures of commercial alloys and the effects of fatigue stressing on these.

The purpose of this paper is to describe the results of an investigation of some microstructural features of the ageing processes and their modification by high and low frequency fatigue in an aluminium-copper alloy of considerable commercial importance, particularly in the aircraft industry.

2. Experimental work

2.1 Material

The alloy used in this work was basically an aluminium-copper alloy in three conditions of heat treatment; solution-treated, optimum aged and overaged, these conditions being those referred to in specifications which are based principally on static mechanical properties. The composition, heat treatments and typical mechanical properties of the alloy are given in Table 1. It should be noted that this alloy forms the basis of over twenty national specifications and is widely used in aircraft structures.

2.2 Fatigue Tests

Fatigue tests were made on specimens at both 50 Hz and 20 kHz at room temperature in the relative humidity range 55 to 75%. Single point cantilever rotating bend machines were used for the 50Hz tests. Axial push-pull 20 kHz tests were made using a magnetostrictively driven resonant system with a combination of acoustic transformers so as to allow the use of plain cylindrical specimens¹². In all fatigue tests the mean stress was zero, specimens were heat treated after machining and had electrolytically polished surfaces.

The lives of specimens in number of cycles to failure for a given stress level were treated as log normally distributed and plotted in the form of stress semi-amplitude against the mean log number of cycles to failure (S - N Curves). A minimum of five tests were made at each of five stress levels. In some high frequency tests, thermocouples were attached to the centres of the specimens at the displacement nodes in order to monitor the temperature changes during the tests.

2.3 Preparation of thin foils

A disc of material, approximately 0.3 mm. thick and 2.3 mm. in diameter, was first produced from bulk material by slitting out a sample from the region of interest and wet grinding through the grades of emery paper, then punching out a disc of the required diameter.

A simple single-stage twin-jet process was used for final thinning.¹³ The electrolyte was a mixture of acetic acid (40%), orthophosphoric acid (30%), nitric acid (20%) and water (10%) which was maintained at a temperature of between -5°C and -12°C at the jets. A current density of about 4 amps/cm² was sufficient to cause perforation within 4 minutes. After washing and drying the specimens were inserted into a Valdre cartridge for examination in a Siemens Elmiskop 1 electron microscope using a 100 kV beam.

3. Results

3.1 Fatigue tests

The fatigue results for the alloy tested are shown in fig.1. Since the stress and specimen geometries of the low and high frequency specimens are not the same, no attempt can be made to compare the S-N curves at the two frequencies. The high frequency tests for the differing heat treatments, whilst indicating a similar life at low stresses, diverge with increasing stress so that the number of cycles to failure at stresses above about 8.5 tonf/in² is greatest for the optimum aged, less for solution treated and least for the overaged material. This is the same order of fatigue strength found in earlier work using specimens of more complex geometry.¹ The low frequency rotating bend results show only slight variation with heat-treatment, the major effect being that the optimum aged material is slightly better at the highest stresses used.

Persistent slip bands were observed on the surfaces of all specimens; these features showed little variation with frequency of cyclic stressing or initial heat treatment condition of the material.

Temperature rises during some tests at high frequency were monitored continuously, and typical curves for each condition of heat treatment are shown in fig. 2 for one stress level only in each case. These indicate that the initial rise in temperature was rapid in all cases but varied with condition. The peak temperature attained at the highest stresses was about 110°C, a rise of about 90°C. Insufficient data are available to draw conclusions on the effect of heat treatment condition on the changes in temperature during the tests.

3.2 Examination of microstructures

3.2.1 Unfatigued material

Intermetallic particles, undissolved during solution treatment, were consistently present in all foils; these were unaffected either by the heat treatments or by fatigue stressing. Three basic types were observed, (a) spherical particles about 0.05μ in diameter, (b) irregular equiaxed particles about 1μ diameter, and (c) irregular elongated particles which appeared to be less absorptive in the electron beam than particles (a) and (b), and which were generally of the order of size of particles (b). Particles (b) and (c) are irregularly distributed whereas (a) particles are fairly uniformly distributed throughout the matrix and grain boundaries.

Figure 3 shows an area in a sample containing examples of all three particles. The smallest particles have been identified in the same alloy by Hershman and Davies¹⁴ and appear to be cubic α (Al Mn Si).

The precipitates formed during ageing have not yet been identified in this study but the nomenclature used to describe them will be in the θ_c sequence¹⁵. It should however be noted that both the intermediate and the equilibrium precipitates may be of the type θ (Al_2Cu), S (Al_2CuMg) or even Mg_2Si . The relatively high proportion of Cu in this alloy tends to support the assumption that a single ageing process takes place and is probably of the θ type modified to some extent by the additional alloying elements.

The precipitates observed were of three basic types. The first, θ''_c , is a coherent orthogonal needle-like structure, comparable in size, shape and form with θ'' in the binary $Al-Cu$ alloy. The second, θ'_c , is partly coherent and appears as rather thicker needles or narrow platelets nucleated on dislocations or grown homogeneously from the θ''_c . The third precipitate takes the form of angular plates which are incoherent and may be either a larger form of θ'_c or θ_c . These equilibrium precipitates showed some association with the smallest of the undissolved intermetallic particles and may be nucleated at the particle/matrix interface.

Figure 4 shows a typical area in solution treated and quenched material. The features were similar to the binary alloy⁷ but the helical dislocations were rather shorter and appeared in many cases to terminate at the smallest of the undissolved intermetallic particles. This gave the appearance of a network of helices with the small particles as nodal points. There were fewer loops than in the $Al-Cu$ binary, and no visible precipitates were observed. After ageing for 5 hours at $180^\circ C$, considerable amounts of θ''_c and some θ'_c were formed, the latter being mainly nucleated on dislocations, giving a step-like appearance. (Figs. 5 and 6). Dislocations were difficult to image owing to the presence of pronounced strain fields around the coherent θ''_c precipitates. (Fig. 7). Overageing for 120 hours at $180^\circ C$ resulted in an increase in the amount of θ'_c , most of which was homogeneously nucleated. Plate like precipitates which were either θ_c or an incoherent form of θ'_c co-existed with both of the intermediate precipitates and there

was some association between the plates and the small undissolved particles. No marked changes were observed in dislocation density or arrangements. Typical structures of the overaged material are shown in Figs. 8 and 9.

3.2.2 Low frequency fatigued material

Fatigue at low frequency of the solution treated material produced no visible precipitates, but there was a considerable increase in the helix concentration, the helices tending to be oriented in preferred directions; Figs. 10 and 11. Some of the foils, when tilted to superimpose extinction fringes on the image, revealed streak markings, as may be seen in Fig. 12. No positive conclusions can be given as to the cause of these markings, but they may be either slip traces or oriented groups of zones. The features characterising these markings are (a) they did not seem either to appear or disappear under the action of the electron beam, (b) if they were slip traces there was no sign of cross slip even when the markings intersected the undissolved particles, (c) the markings extended regularly across the whole grain and (d), as mentioned previously, they were revealed most clearly by superimposition of extinction fringes. Optimum aged material fatigued at low frequency showed both θ''_c and θ'_c the latter being nucleated homogeneously in increased amounts at the expense of θ''_c . (Fig. 13). Short segments of dislocations were present in complex entanglements, but again, these were difficult to image. (Fig. 14). Only a small degree of modification to the precipitates was produced by low frequency stressing of the overaged material. The whole range of precipitates was again observed with possibly a slight increase of homogeneous θ'_c . The dislocation density was also increased by a small amount. These features are seen in Figs. 15 and 16.

3.2.3 High frequency fatigued material

Fatigue at high frequency of the solution treated material produced, as in the low frequency case, a structure showing no evidence of θ''_c precipitates. However, plate like precipitates, tentatively identified as incoherent θ'_c or θ_c , were present in one of the foils again in association with the smallest intermetallic particles; (Fig. 17). There was little change in the helix concentration, but entanglements of short segments of dislocations were evident as shown in Figs. 18 and 19. One area, which was free from the undissolved second phase particles, contained a marked cell structure (Fig. 20). High frequency stressing of the optimum aged material produced more homogeneous θ'_c than did the low frequency testing; there was also some θ_c . (Fig. 21). Dislocations were difficult to image and again no entanglements were observed. The overaged material showed little change after high frequency stressing. (Fig. 22).

The effects observed for all conditions of heat treatment and fatigue are summarised in Table II.

4. Discussion

4.1 Fatigue induced changes in microstructure

The interaction of fatigue stressing with the precipitation processes in age-hardening aluminium alloys has been investigated by a number of workers.^{10, 11} Numerous attempts have been made to account for the relatively poor performance of such materials under alternating stresses and these have tended to fall into three categories.

(a) The overaging hypothesis

Broadly this suggests an acceleration in the ageing process leading to the early formation of semi-coherent or incoherent precipitates with a consequent reduction in mechanical properties. One simple mechanism is that a high local concentration of vacancies may be produced by the non-conservative motion of the oscillating dislocations leading to enhanced diffusion rates. In the case of high-frequency stressing, particularly in the ultrasonic range, an additional factor is the rate of energy dissipation in the material which may lead to a pronounced rise in temperature, again causing an acceleration in the rate of ageing. Hayes and Shyne¹⁶ have recently concluded that in general, high frequency stressing affects ageing processes but little and that experimentally noted effects are mainly due to the heating effect. On the other hand, Brown¹⁷ suggests that greatly accelerated diffusion controlled processes are a consequence of the vibrational stressing itself without reference to temperature changes.

The increased number of dislocations produced during fatigue may also increase diffusion rates locally by providing more 'easy paths' for the solute atoms than is found in the unaged material.

(b) The resolution hypothesis

Kelly and Nicholson⁵ have calculated that provided θ'' coherent precipitates are less than 200Å thick, dislocations can pass through them. Indeed, cutting of these precipitates by dislocations has been observed directly. Various workers have argued on the basis of this cutting mechanism that this could cause resolution of these precipitates provided the local dislocation activity is high enough. It was further proposed that extensive resolution could give rise to precipitate-free areas in which the dislocations could move comparatively easily: bands of high dislocation density could then develop, leading to fatigue failure.

However, this hypothesis has been largely discounted by Laird and Thomas¹¹ who claim, on thermodynamic grounds, that the stability of coherent precipitates remains comparatively unchanged by the increase in precipitate surface due to displacements across the planes on which dislocations are active. These authors concede, however that in some systems such as Fe-C, containing a fine dispersion of carbide particles, resolution may be the preferred mechanism for forming softened regions.

(c) The ageing 'heterogeneity' hypothesis

Although controversy remains on the possibility of fatigue induced resolution, leading to local softening, it has been pointed out¹¹ that many age-hardening aluminium alloys inherently contain zones denuded of coherent precipitates either in specific areas, such as those adjacent to grain boundaries, or as a natural consequence of the ageing process, e.g. in areas around incoherent precipitates that are growing preferentially at the expense of coherent zones or precipitates. With this in mind, it is argued that because plastic deformation accumulates in highly localised areas, there is no need to invoke a resolution mechanism since the alloys invariably contain denuded zones in which bands of high dislocation density can be generated.

4.2 Discussion of results

Dislocation observations

Over 300 foils were examined from specimens which had been subjected to all three conditions of heat treatment and to fatigue stressing at the two frequencies. Despite this, no clearly defined bands of high dislocation density were observed. Fatigue did produce local entanglements of dislocations, but these appeared as formless clumps rather than as high-density banded regions. Linear formations of dislocations were only observed in solution-treated material as helical arrays, as shown in Fig. 12, and as fairly straight dislocations in areas devoid of the undissolved intermetallics (Fig. 23).

It might be argued that since the foils were not taken at the free surface the movement of dislocations in the areas from which the foils were taken would be less intense and hence the propensity for the formation of bands of high dislocation density would be minimised. However, thin foils were also obtained from the interior of a fatigued age-hardening pseudo-binary Al-Cu-Mg alloy, Hyduminium RR58, and bands of high dislocation density were observed frequently. An example is shown in Fig. 24. As RR58 does not contain undissolved intermetallic particles to any great extent, and more particularly, since the material studied in this work reveals linear arrays only in areas free from second-phase particles, it may be concluded that the presence of these particles tends to inhibit the formation of dislocation bands.

Inhomogeneity

Although the undissolved intermetallic particles are fairly uniform in distribution there exist some localised denuded regions inside the grains. Fig. 25 shows such an area. If these regions in the solution treated high frequency fatigued material are tilted to reveal the dislocation arrangements, a cell structure can frequently be seen, indicating that the temperature rise associated with high frequency fatigue is sufficient to polygonize areas denuded of undissolved particles and θ''_c precipitates. (Fig. 21). High

frequency fatigue stressing of commercial-purity aluminium gives rise to a similar effect. (Fig. 26).

Inhomogeneity of the θ_c -type precipitates in the aged materials is not particularly evident. Careful examination of areas adjacent to grain boundaries and around preferentially-growing semi-coherent or incoherent precipitates did not reveal marked denuded zones although, as will be discussed later, equilibrium precipitates which have been grown directly from the solid solution as a consequence of high frequency stressing appeared to be nucleated on the smaller of the undissolved particles; hence the areas in which these are absent tend to be devoid of θ_c (Fig. 27).

Optimum aged material

In the prefatigued state, the microstructure of the optimum aged material consisted mainly of θ_c'' and some dislocation nucleated θ_c' . Fatigue at low frequency increased the amount of θ_c' , which was mainly nucleated homogeneously at the expense of the θ_c'' . This suggests an acceleration in the ageing process. The high frequency fatigued optimum aged material contained even more θ_c' , and indeed some θ_c , pointing to a greater acceleration of the ageing process. This indicates that although the duration of the high frequency tests is much less than the duration of tests at low frequency, the inherent temperature rises in the high frequency specimens increased the rate of diffusion more effectively than that induced solely by room temperature fatigue at the lower frequency.

Dislocations in the optimum aged material were difficult to image and no conclusions can be drawn regarding their density or arrangements.

Overaged material

Neither low nor high frequency fatigue caused very much change to the overaged microstructure. This is consistent with the presence of thermodynamically stable incoherent precipitates in the unfatigued material which are less likely to be affected by dislocation activity.

Examination of the microstructures both before and after fatiguing, provides no adequate reason for the marked differences in performance of the optimum aged and overaged materials during high frequency fatigue and the comparable performance on low frequency stressing.

There is, however, a much higher proportion of what appears to be θ_c'' in the overaged than in the optimum aged material; this is consistently so in both unfatigued and fatigued specimens. Although this is apparently anomalous, it may be due to marked variations in the types and distribution of precipitates and the vagaries existing at this microscopical level of sampling. Alternatively, it is possible that S'' (Al_2CuMg) was present in the overaged microstructure; heat treatment to the optimum aged condition would not be sufficient to nucleate this phase. Again no positive conclusions can be drawn from consideration of the dislocation structures.

Solution treated material

Material freshly solution treated and unfatigued contained no θ_c - type precipitates. Dislocations, mainly helices, were in the form of a network and, in general, emerged at the interface between the matrix and the smallest undissolved particles.

Low frequency stressing caused an increase in the number of helices which, in regions containing few of the undissolved particles, were oriented in specific directions. In areas containing a high proportion of particles there was no apparent alignment and the number of helices was small. It might be supposed, therefore, that the excess vacancies produced locally by moving dislocations combined with the increased numbers of dislocations to form helices which were then anchored by copper atoms from the solid solution. Areas containing a high proportion of undissolved particles provide vacancy sinks at the incoherent interfaces, which may have preferentially absorbed the vacancies produced by fatigue, leaving few to combine with the increased number of dislocations to produce helices.

The zones, or pre-precipitates, may well have been cut by the mobile dislocations, although it is difficult to conclude whether continuous resolution occurred during the fatigue process or whether the zones were simply prevented from growing into visible θ_c'' .

The streak markings, referred to earlier as either slip traces or oriented zones, may provide evidence of dislocation/zone interactions if they are proved to be the latter. One could visualise, for instance, that if dislocation activity is confined to one set of slip planes, then growth of zones would only be possible in parallel planes, since cutting would occur if the zones are aligned in directions other than those that are contained in the (III), as indeed are the zones and precipitates in the θ and S systems. Growth of zones parallel with the slip planes would create considerable lattice distortion and may give rise to diffraction contrast effects such as are seen in Fig. 13.

In the high-frequency fatigued solution-treated material there is evidence in some areas of incoherent θ_c' and/or θ_c , which is somewhat surprising since no θ_c'' was seen. This tends to suggest that the intermediate stages in the ageing process have been bypassed due to a combination of cyclical stress and increased temperature which permits only the growth of incoherent precipitates. The effect of increased temperature and dislocation-produced vacancies is to accelerate the rate of ageing, whereas the effect of cyclical stress is to move the dislocations through the coherent zones, preventing their growth and possibly leading to resolution.

As mentioned previously, examination of these microstructures shows that there is some association between the smaller of the undissolved particles and the equilibrium precipitates, suggesting that nucleation of the θ_c' and/or θ_c occurs at the matrix/particle interface. These sites are

likely to be particularly favoured in fatigued solution treated material because of the increased number of dislocations emerging at the interface. The accelerated growth of these incoherent precipitates causes rapid depletion of copper atoms in solution and provides an increased number of vacancy sinks, thus preventing the formation and anchoring of helices. This is substantiated in these thin foils by an increase only in entanglements, not in helices. Further tests are being made using a Mn-free sample of this alloy in which the $\alpha(\text{AlMnSi})$ particles are absent. Similar experiments will also be made with the Al-Cu-Mg alloy referred to earlier as RR58. In both of these cases the absence of the undissolved intermetallic particles may well show considerably different effects in the solution treated, high frequency fatigued case.

5. Conclusions

For optimum aged alloy samples fatigued at both high and low frequency there was evidence of a slight overageing which was slightly more marked in the high frequency case where there was a temperature rise during test. This is consistent with the overageing hypothesis. On the same basis little effect would have been expected as a result of fatigue of overaged material and indeed this was the case.

Precipitate free zones were not observed in this alloy although there was some heterogeneity in the dispersion of undissolved intermetallic particles.

Regular bands of high dislocation density were not observed with this metal but there were regions of complex entanglements. The arrangements of dislocations in the solution treated material were most markedly affected by fatigue and the resultant structures suggest that it is difficult in these cases for coherent precipitates to grow. Whilst this does not provide evidence for resolution it suggests that the cyclic stress inhibits the growth of G.P. zones and coherent precipitates perhaps by the cutting mechanism invoked in the resolution hypothesis. It seems possible therefore that both accelerated ageing and cutting of zones giving inhibition of the precipitation process can occur simultaneously and indeed none of the hypotheses discussed are necessarily mutually exclusive although in other alloy systems one mechanism may be predominant. No simple explanation, in terms of microstructural changes, can yet be given for the strong effects of heat treatment condition on fatigue life in the high frequency tests nor indeed for the generally poor performance in fatigue of this type of alloy.

Finally, it is clear that the engineering performance of the complex alloy cannot be wholly assessed by tests made only at low frequency, since high frequency stressing can produce more marked changes in microstructure than low frequency stressing. In addition the behaviour of the simple binary alloy and the complex commercial alloy are sufficiently different to reduce the engineering significance of conclusions drawn from examination of the simple alloy.

16. G.A. Hayes and
J.C. Shyne

Metal Science Jnl. 1968, 2, 81.

17. A.F. Brown

Appl. Mats. Research 1966, p. 67.

Table I

Composition	4.4 Cu, 0.7 Si, 0.6 Mg, 0.6 Mn, Balance Al.
Solution treatment	2½ hours at 505°C
Optimum ageing	5 hours at 180°C
Overageing	120 hours at 180°C.

Mechanical Properties

	<u>0.1% Proof Stress</u>	<u>Ultimate Stress</u>	<u>% elongation</u>
Solution treated	17.1 tsi	28.6	17.5
Optimum aged	25.2	31.4	5.8
Overaged	18.1	24.2	10.5

Specifications related to this alloy include 2L62-65.

HEAT TREATMENT	CONDITION	UNFATIGUED	LOW-FREQUENCY FATIGUED (50 Hz)	HIGH-FREQUENCY FATIGUED (20 kHz)
Soak at 505°C Quench in water, (20°C)	SOLUTION TREATED	No visible (Al:Cu) precipitates ----- A network of dislocations, mainly helices, with small undissolved particles at nodal points.	No visible (Al:Cu) precipitates ----- Increased dislocation density, mainly helices, which are aligned in two directions.	Generally, no visible precipitates but a few small areas containing coarse θ'_c and θ_c ----- No increase in number of helices, but some gross dislocation entanglements.
Solution treat then age at 180°C for 5 hours.	OPTIMUM AGED	θ''_c homogeneous and dislocation nucleated θ'_c ----- Fewer dislocations than S. T. (mainly associated with coherent strain fields).	Less θ''_c ; more θ'_c ----- Complex entanglements	More θ'_c ; some θ_c ----- No entanglements (cell structures observed in zones free of undissolved particles).
Solution treat then age at 180°C for 120 hours.	OVERAGED	θ''_c ; θ'_c ; θ_c . (possibly δ'') ----- As optimum aged	Precipitates unmodified by fatigue ----- Increased dislocation density	Precipitates unmodified by fatigue ----- Unmodified

TABLE II

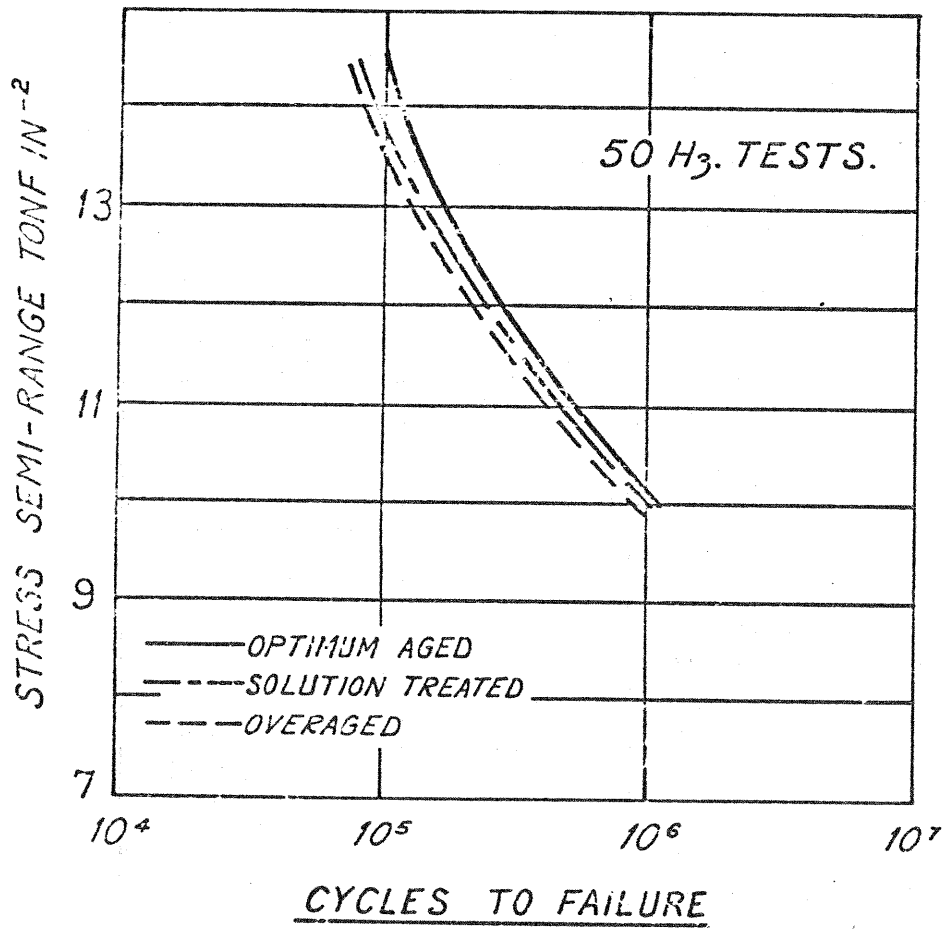
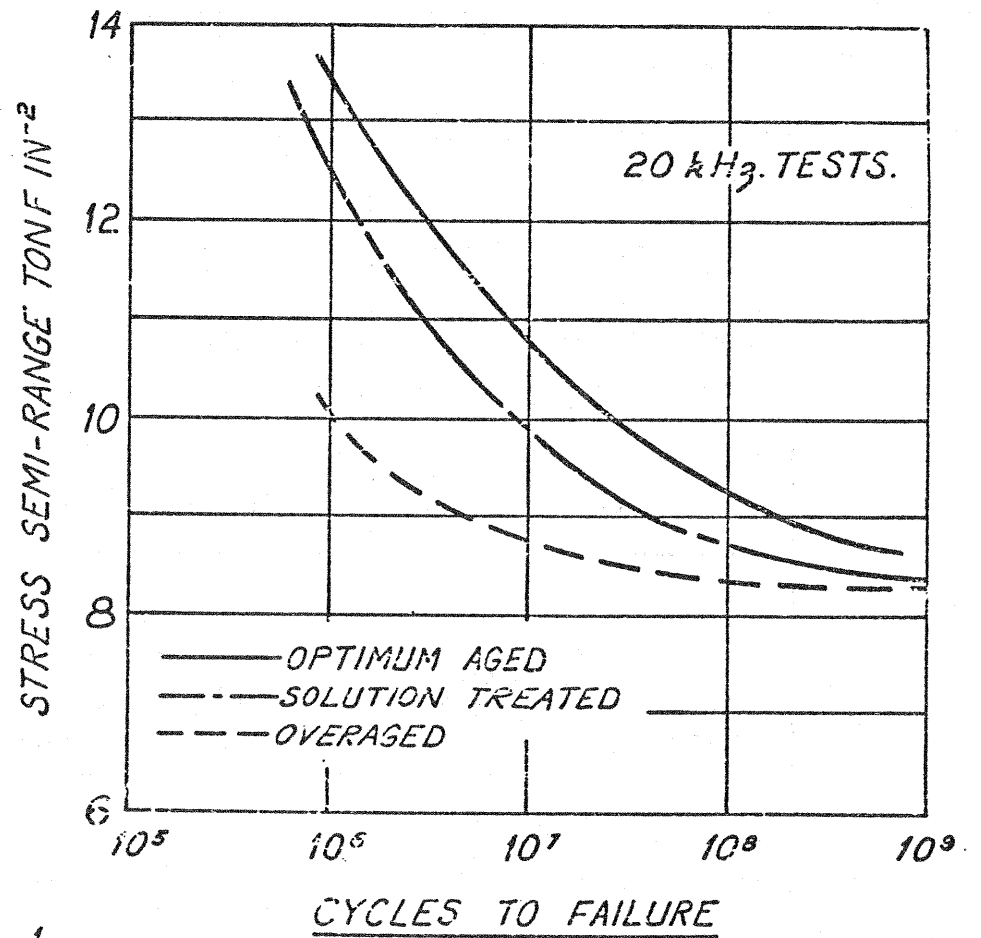


FIG. 1.



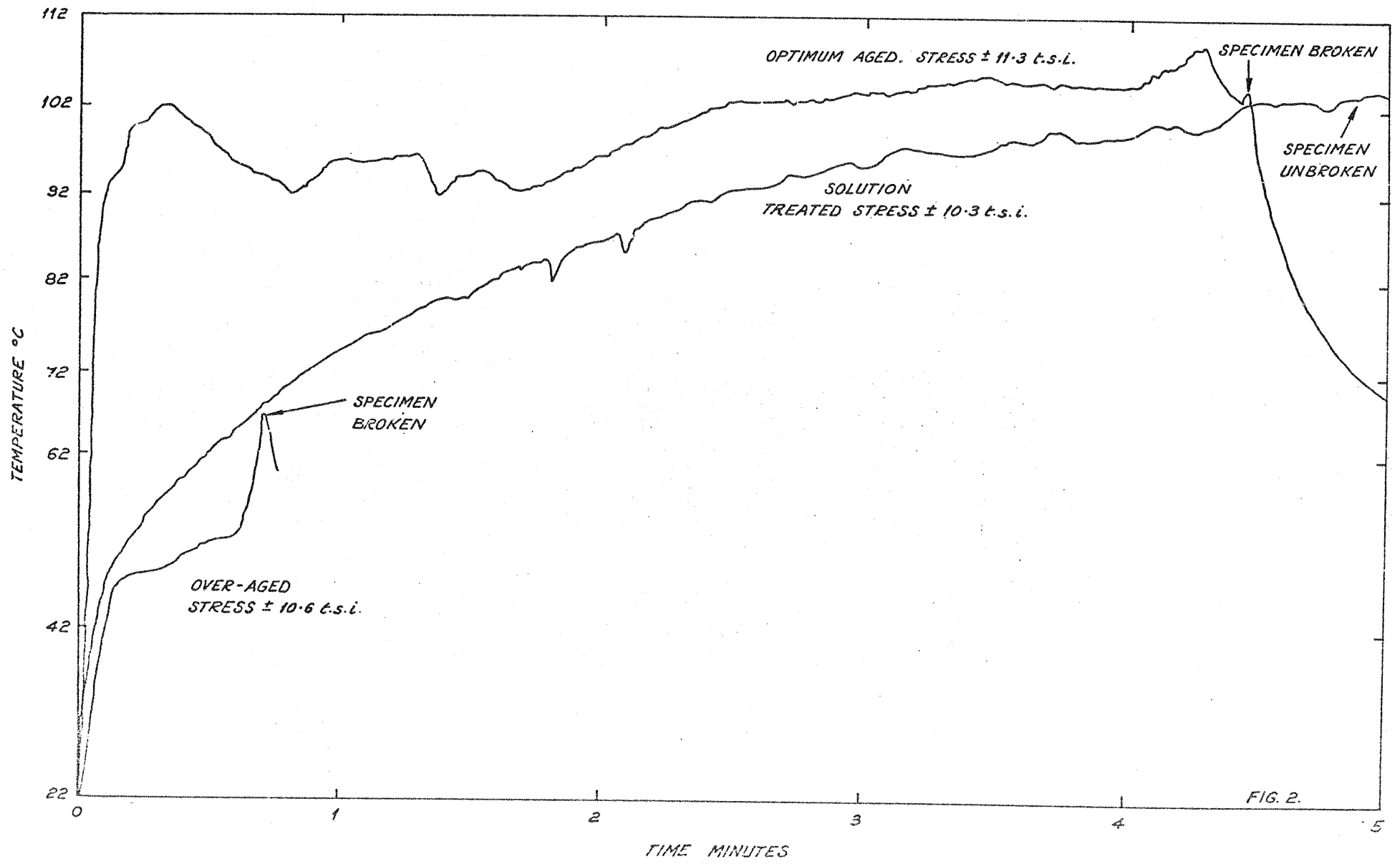


FIG. 2.

FIG. 2.

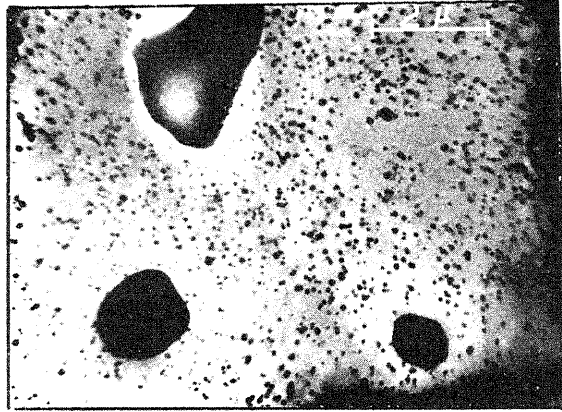


FIG. 3

THE THREE BASIC TYPES OF UNDISSOLVED INTERMETALLIC PARTICLES

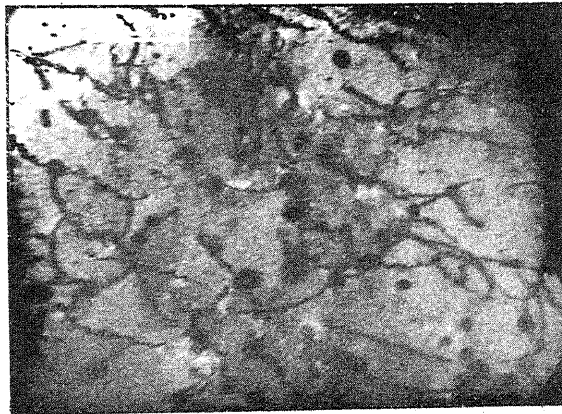


FIG. 4

SOLUTION TREATED UNFATIGUED MATERIAL SHOWING DISLOCATIONS, MAINLY HELICES, TERMINATING AT THE INTERFACE OF THE SMALLEST UNDISSOLVED PARTICLES AND MATRIX.

FIG. 5

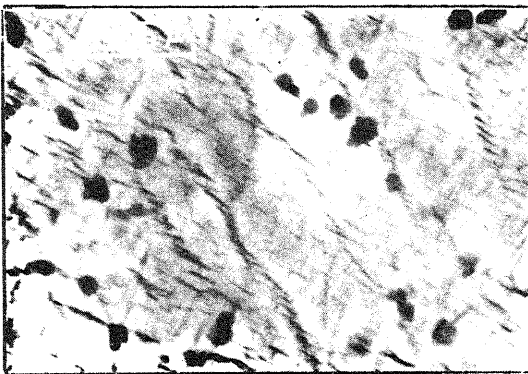
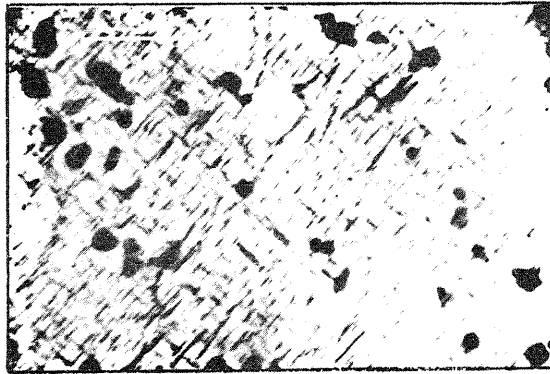


FIG. 6



TWO AREAS OF UNFATIGUED OPTIMUM AGED MATERIAL SHOWING A PREDOMINANCE OF θ'' AND SOME DISLOCATION-NUCLEATED θ'

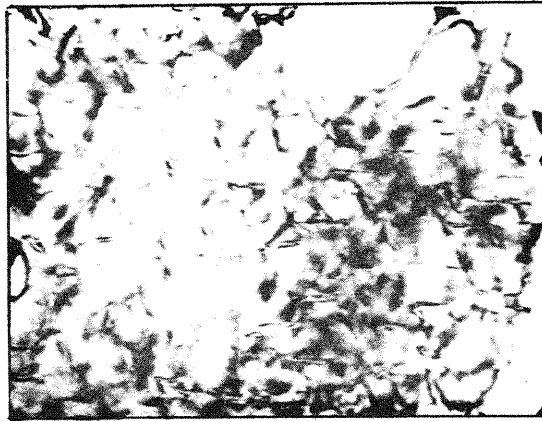
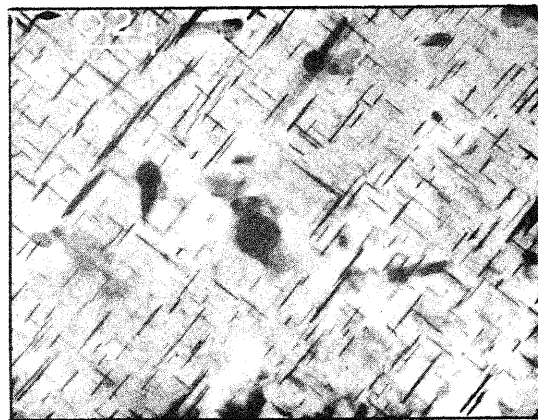
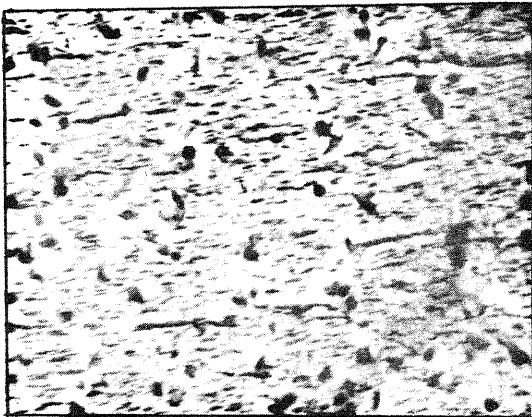


FIG. 7

STRAIN FIELDS AROUND θ'' PRECIPITATES IN UNFATIGUED OPTIMUM AGED MATERIAL

FIG. 8

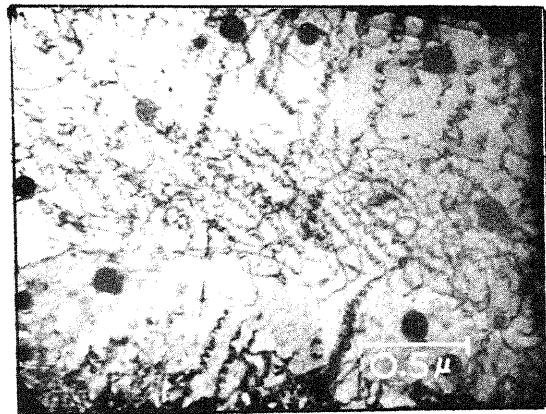
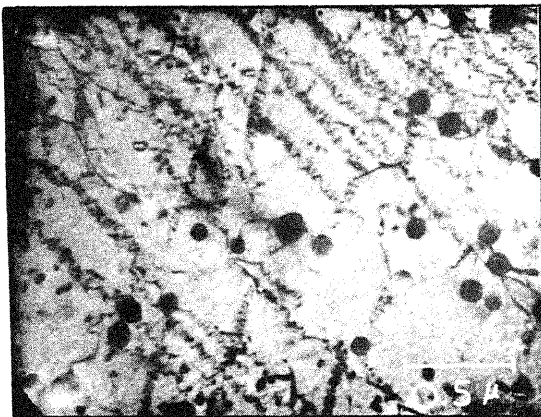
FIG. 9



UNFATIGUED OVERAGED MATERIAL SHOWING A PREDOMINANCE OF HOMOGENEOUS θ'_c AND SOME θ_c . THE NEEDLES IN FIG. 9 MAY BE S' PHASE (Al_2CuMg)

FIG. 10

FIG. 11



TWO AREAS IN THE LOW-FREQUENCY FATIGUED SOLUTION TREATED MATERIAL SHOWING A HIGH DENSITY OF ORIENTED HELICAL DISLOCATIONS.

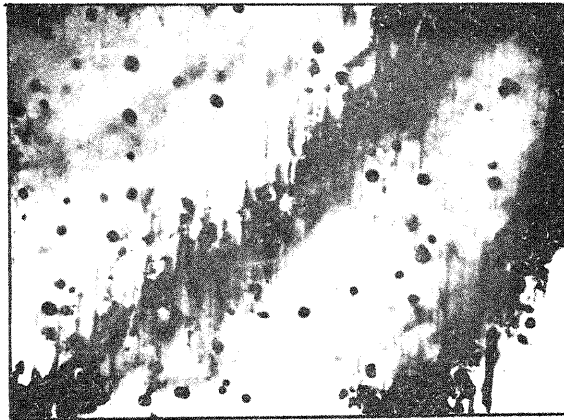
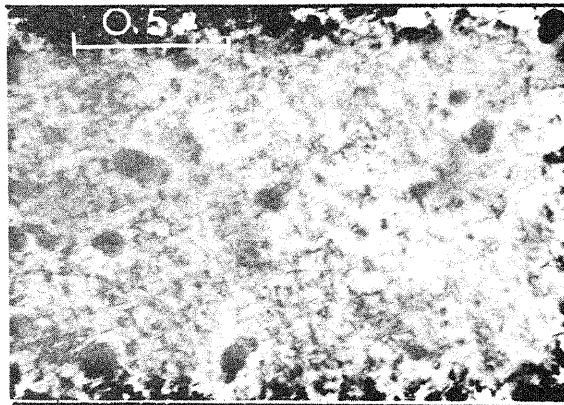
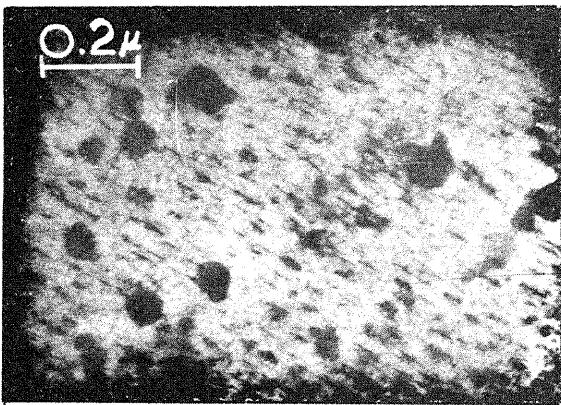


FIG. 12

STREAK MARKINGS REVEALED BY EXTINCTION FRINGES. SOLUTION TREATED LOW-FREQUENCY FATIGUED MATERIAL.

FIG. 13

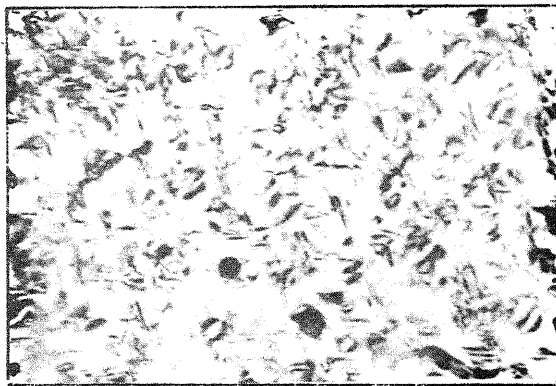
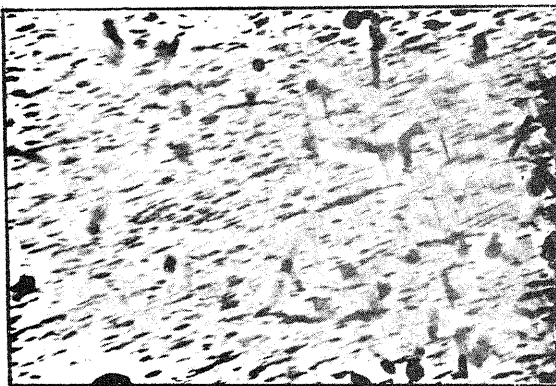
FIG. 14



OPTIMUM AGED MATERIAL FATIGUED AT LOW FREQUENCY SHOWING MAINLY HOMOGENEOUS θ' . COHERENT STRAIN FIELDS CAN BE SEEN IN FIG. 14

FIG. 15

FIG. 16



LOW-FREQUENCY FATIGUED OVERAGED MATERIAL. FIG. 15 SHOWS θ' AND θ AND FIG. 16 REVEALS STRAIN FIELDS SURROUNDING COHERENT PRECIPITATES.

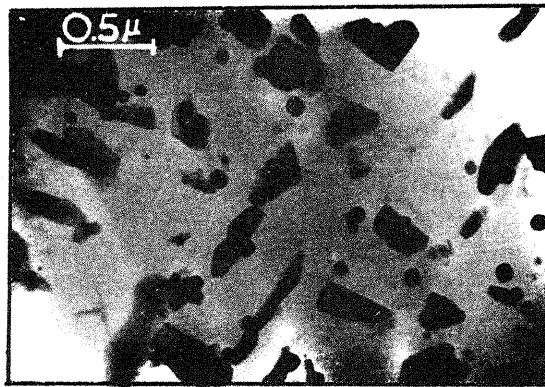
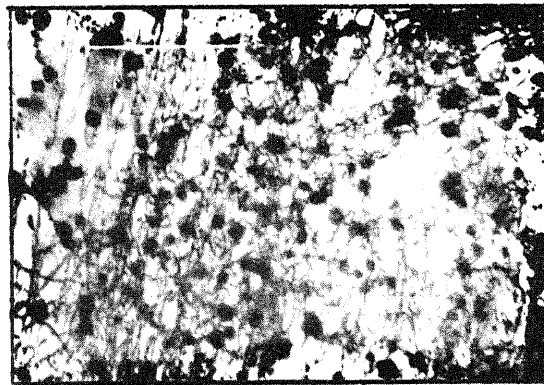
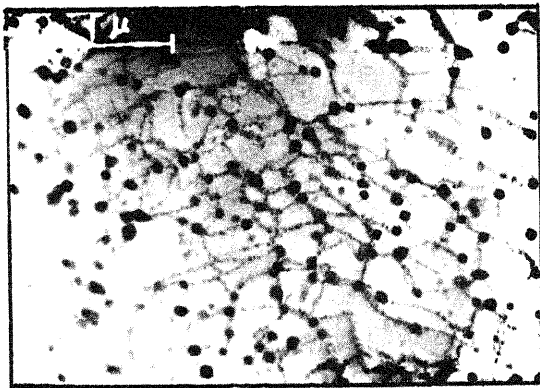


FIG. 17

θ_c AND/OR θ'_c IN THE SOLUTION TREATED HIGH-FREQUENCY FATIGUED MATERIAL.

FIG. 18

FIG. 19



TWO AREAS IN HIGH-FREQUENCY FATIGUED SOLUTION TREATED MATERIAL SHOWING NO MULTIPLICATION OF HELICES (FIG. 18), BUT AN INCREASE LOCALLY OF DISLOCATION ENTANGLEMENTS (FIG. 19)

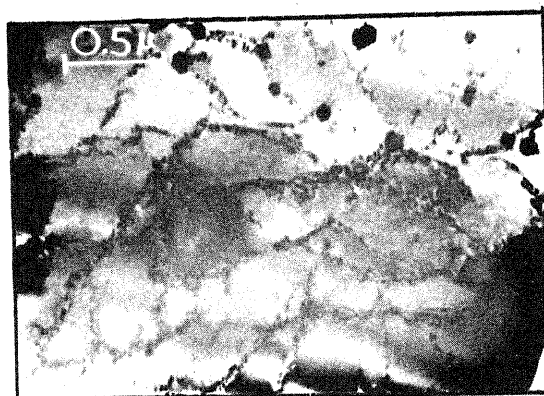


FIG. 20

SOLUTION TREATED HIGH-FREQUENCY FATIGUED MATERIAL SHOWING AN AREA DENUDED OF UNDISSOLVED INTERMETALLICS IN WHICH A POLYGONIZED DISLOCATION STRUCTURE IS APPARENT.

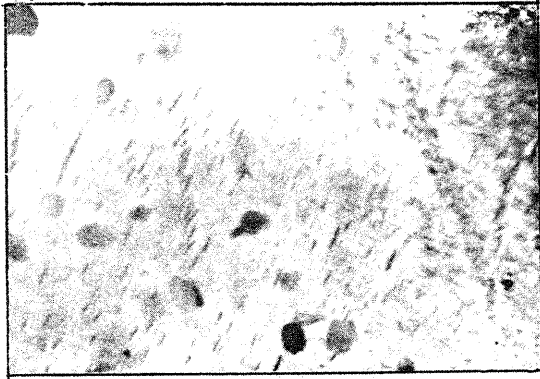


FIG. 21
 θ'_c AND θ_c IN HIGH-FREQUENCY
 FATIGUED OPTIMUM AGED MATERIAL.

FIG. 22
 HIGH-FREQUENCY FATIGUED OVERAGED
 MATERIAL. THIS SHOWS θ_c , θ'_c
 AND EITHER θ''_c OR S' .

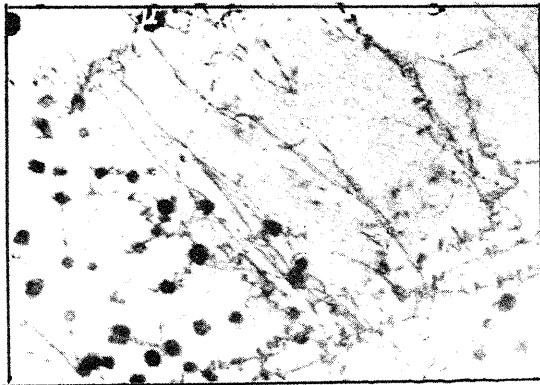
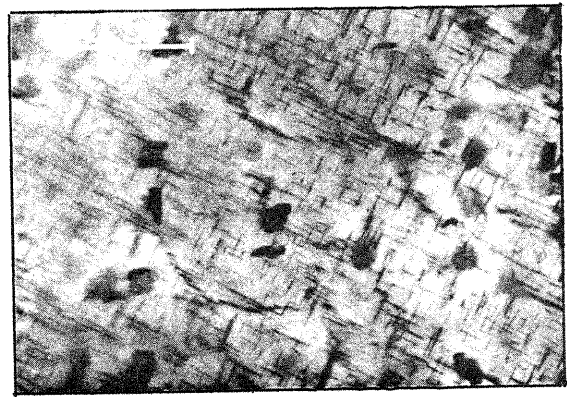
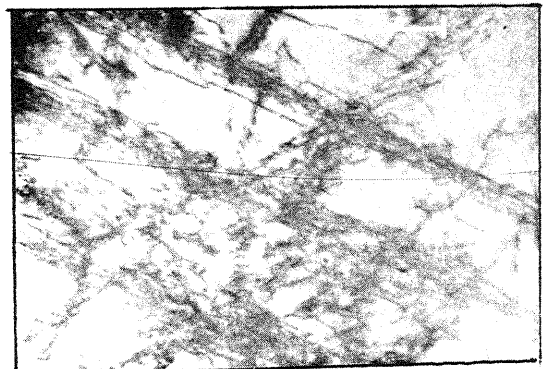


FIG. 23
 STRAIGHT DISLOCATIONS IN A
 REGION FREE FROM INTERMETALLIC
 PARTICLES. SOLUTION TREATED
 HIGH-FREQUENCY FATIGUED
 MATERIAL.

FIG. 24
 WELL DEVELOPED BANDS OF
 DISLOCATIONS IN HIGH-FREQUENCY
 FATIGUED RR58.



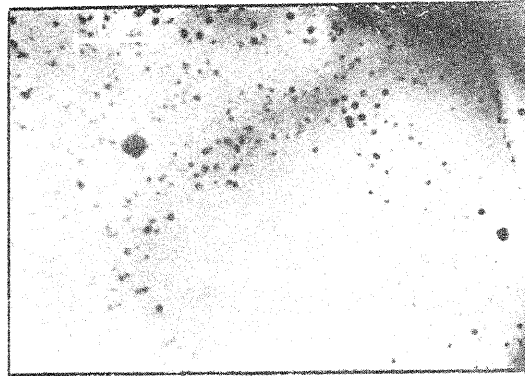


FIG. 25 SOLUTION TREATED MATERIAL SHOWING AN AREA FREE FROM UNDISSOLVED INTERMETALLIC PARTICLES.

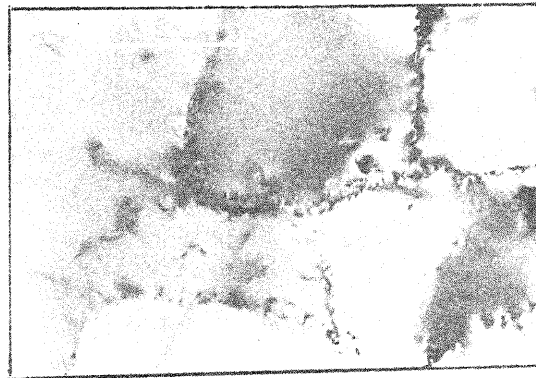


FIG. 26 HIGH-FREQUENCY FATIGUED COMMERCIAL-PURITY ALUMINIUM. FATIGUE, PLUS A TEMPERATURE RISE ASSOCIATED WITH HIGH-FREQUENCY STRESSING, HAS RESULTED IN EXTENSIVE POLYGONIZATION. COMPARE THIS PHOTOMICROGRAPH WITH FIG. 20.



FIG. 27 HIGH-FREQUENCY FATIGUED SOLUTION TREATED MATERIAL. AREAS DEVOID OF UNDISSOLVED PARTICLES DO NOT SHOW θ_c AFTER STRESSING AT 20kHz. THIS CORRESPONDENCE BETWEEN THE EQUILIBRIUM PHASE AND THE PARTICLES INDICATES THAT θ_c IS NUCLEATED AT THE MATRIX/PARTICLE INTERFACE.